

UV and IR Spectroscopy of Cold 1,2-Dimethoxybenzene Complexes with Alkali Metal Ions

Yoshiya Inokuchi,^{‡,*} Oleg V. Boyarkin,[†] Takayuki Ebata,[‡] and Thomas R. Rizzo^{†,*}

*Department of Chemistry, Graduate School of Science, Hiroshima University,
Higashi-Hiroshima, Hiroshima 739-8526, Japan and Laboratoire de Chimie Physique
Moléculaire, École Polytechnique Fédérale de Lausanne, Lausanne CH-1015,
Switzerland*

Abstract

We report UV photodissociation (UVPD) and IR-UV double-resonance spectra of 1,2-dimethoxybenzene (DMB) complexes with alkali metal ions, $M^+\bullet\text{DMB}$ ($M = \text{Li}, \text{Na}, \text{K}, \text{Rb}, \text{and Cs}$), in a cold, 22-pole ion trap. The UVPD spectrum of the Li^+ complex shows a strong origin band. For the $\text{K}^+\bullet\text{DMB}$, $\text{Rb}^+\bullet\text{DMB}$, and $\text{Cs}^+\bullet\text{DMB}$ complexes, the origin band is very weak and low-frequency progressions are much more extensive than that of the Li^+ ion. In the case of the $\text{Na}^+\bullet\text{DMB}$ complex, spectral features are similar to those of the K^+ , Rb^+ , and Cs^+ complexes, but vibronic bands are not resolved. Geometry optimization with density functional theory indicates that the metal ions are bonded to the oxygen atoms in all the $M^+\bullet\text{DMB}$ complexes. For the Li^+ complex in the S_0 state, the Li^+ ion is located in the same plane as the benzene ring, while the Na^+ , K^+ , Rb^+ , and Cs^+ ions are off from the plane. In the S_1 state, the Li^+ complex has a structure similar to that in the S_0 state, providing the strong origin band in

the UV spectrum. In contrast, the other complexes show a large structural change to the out-of-plane direction upon S_1-S_0 excitation, which results in the extensive low-frequency progressions in the UVPD spectra. For the $\text{Na}^+\bullet\text{DMB}$ complex, fast charge transfer occurs from Na^+ to DMB after the UV excitation, making the bandwidth of the UVPD spectrum much broader than that of the other complexes and producing photofragment DMB^+ ion.

*To whom correspondence should be addressed. E-mail:
y-inokuchi@hiroshima-u.ac.jp (YI), thomas.rizzo@epfl.ch (TRR).

‡Hiroshima University

†École Polytechnique Fédérale de Lausanne

1. Introduction

This report is a part of our studies on gas-phase spectroscopy of cold benzo-crown ether complexes with metal ions.¹ Crown ethers have been extensively used in host-guest chemistry because of selective encapsulation of metal ions. One of the methods to verify complex formation of crown ethers in solution was UV spectroscopy.² However, a broad nature of UV spectra due to solvent and temperature effect makes it difficult to determine the complex structure in solution. X-ray structural analysis of crystals is also quite useful, but metal cations are often coordinated not only by crown ethers but by counter anions in crystals, which significantly changes the complex structure.³⁻⁸ UV and IR spectroscopic studies of jet-cooled benzo-crown ethers and their complexes with neutral species have provided information on the ether conformation.⁹⁻¹³ Recently, we have measured UV spectra of cold dibenzo-18-crown-6 (DB18C6) complexes with alkali metal ions, $M^+\bullet\text{DB18C6}$ ($M = \text{Li, Na, K, Rb, and Cs}$) by UV photodissociation (UVPD) spectroscopy.¹ Thanks to a cold 22-pole ion trap, the UVPD spectra show a number of sharp bands, which make it possible to determine the number and the structure of conformers.^{1,14-16} In the UV spectra of the $\text{Li}^+\bullet\text{DB18C6}$ and $\text{Na}^+\bullet\text{DB18C6}$ complexes, the origin band is very weak, followed by extensive and intense low-frequency progressions. These spectral features suggest a large conformation change upon UV excitation.

In this study, we report UVPD spectra of 1,2-dimethoxybenzene (DMB) complexes with alkali metal ions, $M^+\bullet\text{DMB}$ ($M = \text{Li, Na, K, Rb, and Cs}$) as model systems of alkali metal ion-benzo-crown ether complexes. Measurement of UV spectra and determination of the structure of the $M^+\bullet\text{DMB}$ complexes will provide information on the relation between UV spectral features and the complex conformation. The $M^+\bullet\text{DMB}$ complexes are produced by nanoelectrospray, mass-selected by a

quadrupole mass spectrometer, and irradiated with a UV laser in a cold 22-pole ion trap. In the ion trap, the complexes are cooled down to ~ 10 K.¹⁴⁻¹⁶ We also measure IR-UV double-resonance spectra of the $M^+\bullet$ DMB complexes in the CH stretching region. The structure of the $M^+\bullet$ DMB complexes is determined with the aid of quantum chemical calculations.

2. Experimental and computational methods

The details of the experiment have been given elsewhere.^{1, 14} Briefly, the $M^+\bullet$ DMB ($M = \text{Li, Na, K, Rb, and Cs}$) complexes are produced at atmospheric pressure using nanoelectrospray with $200 \mu\text{M}$ solutions of DMB and metal chloride salts in methanol. Ions are drawn into vacuum by a metal-coated glass capillary. After passing through a 1 mm diameter skimmer, ions are collected for ~ 100 ms in a hexapole ion trap. Once released from the hexapole, the ion packet passes through a quadrupole mass filter to select those of a particular m/Z . The transmitted ions are then turned 90° by a static quadrupole deflector, decelerated by a series of lenses and guided by an octopole ion guide into a 22-pole ion trap, which is cooled to ~ 4 K by a closed-cycle He refrigerator. The He gas is injected into the trap volume using a pulsed valve. The ions in the trap are cooled internally and translationally to low temperature through collisions with cold He buffer gas. The vibrational temperature of trapped ions is estimated to be ~ 10 K.¹⁴⁻¹⁶ We introduce a UV laser pulse from a frequency-doubled dye laser to the axis of the 22-pole ion trap, promoting the complexes to the S_1 state, from which some fractions of them dissociate. Both parent and fragment ions are released from the trap, turned 90° in a second static quadrupole and passed through an analyzing quadrupole to select an m/Z of a particular fragment ion. The transmitted ions are then detected by a channeltron electron multiplier. UVPD spectra are measured by recording the signal of a particular fragment ion as a function of the

wavenumber of the UV laser. Although all the $M^+\bullet\text{DMB}$ complexes provide a few kinds of fragment ions under the irradiation of the UV laser, features of the UVPD spectra do not depend on fragment ions monitored. For IR-UV double-resonance spectroscopy, we use a tunable IR OPO laser (LaserVision) pumped with a Nd:YAG laser. An output of the IR laser is coaxially introduced with the UV laser ~ 100 ns prior to the UV pulse. The wavenumber of the UV laser is fixed to a particular vibronic band in the UVPD spectra for monitoring the population of the zero-point level of a conformer. The wavenumber of the IR laser is scanned while monitoring fragment ion intensity induced by the UV laser. IR-UV spectra are obtained by plotting the yield of a particular photofragment ion as a function of the wavenumber of the IR laser.

Quantum chemical calculations of the $M^+\bullet\text{DMB}$ complexes are carried out with the GAUSSIAN 09 program package.¹⁷ Geometry optimization and vibrational analysis in the S_0 state are done at the M05-2X/6-31+G(d) level of theory. We also perform geometry optimization in the S_1 state with time-dependent density functional theory (TD-DFT) at the M05-2X/6-31+G(d) level; optimized structures in the S_0 state are used as initial geometries for the S_1 optimization. For Rb and Cs, Stuttgart RLC effective core potentials (ECPs) are used; functions of the ECPs are obtained from a database of basis sets.¹⁸

3. Results and discussion

3.1. UV spectra

Figure 1 shows the UVPD spectra of the $M^+\bullet\text{DMB}$ ($M = \text{Li}, \text{Na}, \text{K}, \text{Rb},$ and Cs) complexes with an LIF spectrum of jet-cooled DMB measured by Pratt and coworkers.¹⁹ The UV excitation of the $\text{K}^+, \text{Rb}^+,$ and Cs^+ complexes produces M^+ and $(M\bullet\text{C}_6\text{H}_4\text{OCH}_3\text{O})^+$ fragment ions. In the case of the $\text{Li}^+\bullet\text{DMB}$ complex,

$(\text{Li}\cdot\text{C}_6\text{H}_4\text{OCH}_3\text{O})^+$ and $(\text{Li}\cdot\text{C}_6\text{H}_4\text{O}_2)^+$ fragments are found; Li^+ ion ($m/Z = 7$) cannot be detected with the second quadrupole mass filter because of its low-mass cut off. The UVPD spectra of the Li^+ , K^+ , Rb^+ , and Cs^+ complexes in Fig. 1 are measured by detecting the $(\text{M}\cdot\text{C}_6\text{H}_4\text{OCH}_3\text{O})^+$ ion. For the UVPD spectrum of the $\text{Na}^+\cdot\text{DMB}$ complex in Fig. 1b, DMB^+ ion is detected as a photofragment; the photofragmentation process characteristic of the Na^+ complex is discussed later. All the $\text{M}^+\cdot\text{DMB}$ complexes show a blue shift of the absorption relative to that of bare DMB. In the UV spectroscopic study of $\text{DMB}\cdot\text{H}_2\text{O}$ complex it was reported that the formation of intermolecular bonds between the oxygen atoms of DMB and the hydrogen atoms of H_2O through $\text{O}\cdots\text{H}\cdots\text{O}$ hydrogen bonds shifts the absorption to the blue.¹⁹ Therefore, the metal ions in the $\text{M}^+\cdot\text{DMB}$ complexes are bonded to the oxygen atoms of DMB. The Li^+ complex shows the most blue-shifted band origin, indicating the strongest interaction.

The $\text{M}^+\cdot\text{DMB}$ complexes have spectral features different from each other. The $\text{Li}^+\cdot\text{DMB}$ complex has a strong origin band at 37248 cm^{-1} , accompanied by weaker vibronic bands. For the other complexes, the origin band is too weak to be identified. Figure 2 is enlarged views of the UVPD spectra of the K^+ , Rb^+ , and Cs^+ complexes. Different from the Li^+ spectrum, the spectra show more extensive activity of low-frequency progressions. The interval between the bands gradually decreases from 21.6 to 14.3 cm^{-1} for $\text{K}^+\cdot\text{DMB}$ and from 15.0 to 9.7 cm^{-1} for $\text{Rb}^+\cdot\text{DMB}$ from low to high UV wavenumber, because of an anharmonic nature of the low-frequency vibrations. For the Cs^+ complex, the expanded view in Fig. 2c shows many humps with an interval of 9.5 cm^{-1} ; the broadness of the Cs^+ spectrum is probably due to spectral congestion with very low-frequency progressions. The spectral features of the $\text{Na}^+\cdot\text{DMB}$ complex are similar to those of the K^+ , Rb^+ , and Cs^+ complexes. However,

we cannot find any regular pattern in the Na⁺ spectrum. The weakness of the origin band and the extensive low-frequency progressions observed for the Na⁺, K⁺, Rb⁺, and Cs⁺ complexes indicate that these complexes experience a large structural change upon S₁-S₀ excitation along to the coordinate of low-frequency normal modes.

3.2. IR spectra

Figure 3 displays the IR-UV spectra of the M⁺•DMB complexes in the CH stretching (2800–3120 cm⁻¹) region with stick IR spectra calculated for optimized structures. Calculated frequencies are multiplied by a scaling factor of 0.930 for comparison with the IR-UV spectra. For the Li⁺•DMB complex, only a weak band is observed at 3027 cm⁻¹. The highest-frequency bands move to the red from 3027 (Li⁺•DMB), 3010 (Na⁺•DMB), to 3001 cm⁻¹ (K⁺•DMB), but the band position does not change so much for Rb⁺•DMB (2996 cm⁻¹) and Cs⁺•DMB (2995 cm⁻¹). This result suggests that the interaction between the M⁺ ion and the DMB component becomes progressively weaker from Li⁺ to K⁺. In the IR-UV spectra, the depth of the depletion becomes deeper with increasing the ion size from Li⁺ to Cs⁺. This tendency is reproduced in the calculated spectra. In the region of the CH stretching vibration, there are three strong IR bands, which are attributed to the methyl groups. The intensity of the three IR bands becomes stronger with increasing the ion size. As clearly seen in the Cs⁺ case, the IR-UV spectrum shows more than three IR bands. Poor agreement in the number and the position of the IR bands between the experimental and the theoretical spectra can be ascribed to the Fermi resonance interaction between the CH stretching and the overtone of the CH bending.¹

3.3. Complex structure

We analyze the UV spectra and determine the structure of the $M^+\bullet$ DMB complexes with the aid of DFT calculations. Figure 4 shows the structure of the $Li^+\bullet$ DMB complex in the S_0 state optimized at the M05-2X/6-31+G(d) level. The Li^+ ion is bonded to the oxygen atoms, and the dihedral angles of C3–C2–O9–C10 and C6–C1–O7–C8 are 0 degree, giving a C_{2v} structure. Figure 5 shows side views of the optimized structures for the Li^+ , Na^+ , and K^+ complexes in the S_0 and S_1 states. The distance from the plane of benzene to the M atom, O–M distance (L), and dihedral angle of C3–C2–O9–C10 (θ) are collected in Table 1. In all the stable structures the metal ions are bonded to the oxygen atoms. In the S_0 state, the Li^+ ion is located in the plane of the benzene ring. The Na^+ , K^+ , Rb^+ , and Cs^+ complexes have the metal ions apart from the benzene plane (0.13–1.16 Å) and the dihedral angle is not zero (3.1–21.2 degree).

Geometry optimization in the S_1 state demonstrates that there is large difference in the stable form between the S_0 and S_1 states for the Na^+ , K^+ , Rb^+ , and Cs^+ complexes. As seen in Fig. 5 and Table 1, the Li^+ complex in the S_1 state has a similar C_{2v} structure to that in the S_0 state. In contrast, the Na^+ , K^+ , Rb^+ , and Cs^+ complexes have a large structural change between S_0 and S_1 to the out-of-plane direction of the benzene ring. The dihedral angle θ becomes smaller from the S_0 to S_1 states, indicating that the DMB component prefers to have a planar form ($\theta = 0$) in the S_1 state. This can be confirmed with the UV spectra of bare DMB (Fig. 1f) and the $M^+\bullet$ DMB complexes.¹⁹ Bare DMB and the $Li^+\bullet$ DMB complex have a planar structure in the S_0 state. Since the structural change is small between the S_0 and S_1 states, they show the strong origin band and less activity of low-frequency progressions in the UV spectra.

In contrast, the $M^+\bullet\text{DMB}$ ($M = \text{Na}, \text{K}, \text{Rb}, \text{and Cs}$) complexes have distorted forms in the S_0 state. Therefore, these complexes have very weak origin band and substantial low-frequency progressions in the UVPD spectra. Figure 6 displays the lowest-frequency vibration (19 cm^{-1}) of the $\text{Na}^+\bullet\text{DMB}$ complex in the S_0 state. The Na^+ ion goes to the out-of-plane direction of the benzene ring, followed by the methoxy groups moving to the opposite direction. All the complexes of Na^+ , K^+ , Rb^+ , and Cs^+ have a similar out-of-plane vibration. The out-of-plane torsional vibrations of the methoxy groups are probably involved in the extensive progressions in the UV spectra.

Table 2 shows the binding energy in the S_0 and S_1 states and transition energy calculated for the $M^+\bullet\text{DMB}$ complexes at the M05-2X/6-31+G(d) level. Our study on UVPD spectroscopy of benzo-crown ether complexes with alkali metal ions indicates that the stronger the interaction between the metal ions and the oxygen atoms is, the higher the S_1 - S_0 transition energy is.¹ A similar trend is seen also for the $M^+\bullet\text{DMB}$ complexes. The calculated transition energy is highest for the Li^+ complex and decreases progressively from Li^+ to Cs^+ . This trend agrees with the decrease of the binding energy in the S_0 state from Li^+ to Cs^+ . For the Li^+ complex, the binding energy in the S_1 state is smaller than that in the S_0 state, which is consistent with the UVPD result that the origin band of the Li^+ complex shifts to the blue from the position of DMB monomer. For the other $M^+\bullet\text{DMB}$ complexes, however, the binding energy in the S_1 state is not necessarily smaller than that in the S_0 state; the Na^+ and K^+ complexes have higher binding energies in S_1 than those in S_0 . This suggests that the blue shift of the UV transition for the $M^+\bullet\text{DMB}$ ($M = \text{Na}, \text{K}, \text{Rb}, \text{and Cs}$) complexes results to some extent from the transition nature of these complexes that the potential minima in the S_1 state are not accessible from the minima in the S_0 state, which is

derived from the spectral features that the origin band is not identified and extensive low-frequency progressions are observed.

The preference of a planar form of DMB in the S_1 state is related to the conformation change of the $M^+\bullet\text{DB18C6}$ complexes upon UV irradiation.¹ The $M^+\bullet\text{DB18C6}$ complexes with $M = \text{Li}$ and Na have a highly distorted structure in the S_0 state. The DMB parts ($\text{C}-\text{O}-\text{C}_6\text{H}_4-\text{O}-\text{C}$) of DB18C6 prefer to have a planar form in the S_1 state, which causes the opening of the ether ring upon S_1-S_0 excitation. As a result, the $M^+\bullet\text{DB18C6}$ complexes with $M = \text{Li}$ and Na show extensive low-frequency progressions in the UV spectra.¹

3.4. UV photodissociation process of $\text{Na}^+\bullet\text{DMB}$

As mentioned above, the $\text{Na}^+\bullet\text{DMB}$ complex produces DMB^+ ion as a photofragment. In addition, the UVPD spectrum of the Na^+ complex shows broad features. All these observations can be ascribed to fast charge transfer (CT) from the Na^+ ion to the DMB component after the UV excitation. Figure 7 displays fragment mass spectra of the $\text{Na}^+\bullet\text{DMB}$ ion with (solid curve) and with no (dotted curve) UV laser. The signal at $m/Z = 138$ is assigned to DMB^+ ion. Ionization potential (IP) of Na and DMB was reported as 5.14 and 7.80 eV, respectively; most of the positive charge in the $\text{Na}^+\bullet\text{DMB}$ complex is probably localized on the Na component.²⁰ Therefore, the fragment DMB^+ ion is produced via a charge transfer process from Na^+ to DMB after the UV excitation. Photofragment signals at $m/Z = 123$ and 95 correspond to $(\text{Na} + \text{CH}_3)$ and $(\text{Na} + \text{C}_2\text{H}_3\text{O})$ loss, respectively. Dissociation of CH_3 and $\text{C}_2\text{H}_3\text{O}$ from DMB^+ was also observed in electron-impact ionization of DMB .²¹ The broad features in the UV spectrum of $\text{Na}^+\bullet\text{DMB}$ are attributed to short lifetime in the S_1 state due to fast charge transfer. Figure 8 presents an energy diagram of the $\text{Na}^+\bullet\text{DMB}$

complex and related species. The origin of the vertical axis in Fig. 8 is the summation of the energy of Na and DMB. The difference in IP between Na and DMB is 2.66 eV.²⁰ The binding energy between Na⁺ and DMB is estimated as 1.82 eV from results of our calculations. The S₁-S₀ transition energy observed for the Na⁺•DMB complex is ~4.59 eV (~37000 cm⁻¹). As seen in Fig. 8, the S₁ energy level of the Na⁺•DMB complex is above the dissociation limit of (Na + DMB⁺). After the UV excitation of the Na⁺•DMB complex, fast internal conversion occurs from the potential of Na⁺•DMB (S₁) to the one correlating to the (Na + DMB⁺) dissociation limit. As a result, the photofragment DMB⁺ ion is produced from the Na⁺•DMB complex. Photodissociation mechanism of the M⁺•DMB complexes is controlled by the energetics of the electronic states and the dissociation limits.

4. Summary

We have measured the UV photodissociation (UVPD) spectra of the complexes of 1,2-dimethoxybenzene (DMB) with alkali metal ions, M⁺•DMB (M = Li, Na, K, Rb, and Cs) produced by nanoelectrospray and cooled down to ~10 K in the cold 22-pole ion trap. The Li⁺, K⁺, and Rb⁺ complexes show many well-resolved sharp bands, but the vibronic structure of the Li⁺ one is quite different from the others. In the UVPD spectrum of the Li⁺ complex the origin band is strong, while it is too weak to be identified in the UV spectra of the K⁺, Rb⁺, and Cs⁺ complexes. For these complexes, the low-frequency progressions are more extensive than that of the Li⁺ ion. The Na⁺•DMB complex also has spectral features similar to those of K⁺•DMB, Rb⁺•DMB, and Cs⁺•DMB, but the vibronic bands are not resolved. We have analyzed the UVPD spectra and determined the structure of the complexes with the DFT calculations. In the S₀ state, the Li⁺ complex has a planar structure in which the metal ion is bonded to the oxygen atoms and located in the same plane as the benzene ring. In the Na⁺, K⁺,

Rb⁺, and Cs⁺ complexes, the metal ions are located off from the benzene plane. In the S₁ state, the structure of the Li⁺ complex is almost the same as that in the S₀ state. In contrast, the other complexes experience a large structural change to the out-of-plane direction of the benzene ring upon UV excitation. This results in the extensive low-frequency progressions observed in the UVPD spectra. For the Na⁺ complex, fast charge transfer occurs from Na⁺ to DMB after the UV excitation, producing photofragment DMB⁺ ion and making the bandwidth of the absorption much broader than that of the other complexes.

Acknowledgment

This work is supported by Grant-in-Aids (Grant No. 21350016) for Scientific Research from the Ministry of Education, Culture, Sports, Science, and Technology (MEXT) of Japan and the Swiss National Science foundation through grant 200020_130579. TE thanks the support of MEXT for the Scientific Research on Priority Area “Molecular Science for Supra Functional Systems “ (No. 477). YI also thanks the support from the Excellent Young Researchers Overseas Visit Program of Japan Society for the Promotion of Science (JSPS).

Table 1. Distance between M^+ and benzene plane, O– M^+ distance L , and dihedral angle θ of the $M^+\cdot$ DMB complexes optimized at the M05-2X/6-31+G(d) level with Stuttgart RLC potential for Rb and Cs.

M^+	Distance between M^+ and benzene plane (Å)		O–M distance L (Å)		Dihedral angle θ (degree)	
	S_0	S_1	S_0	S_1	S_0	S_1
Li ⁺	0.00	0.00	1.85	1.86	0.0	0.0
Na ⁺	0.13	1.37	2.22	4.11	3.1	2.3
K ⁺	0.86	2.36	2.63	4.87	15.0	0.1
Rb ⁺	1.12	0.47	2.89	2.94	19.9	16.8
Cs ⁺	1.16	0.65	3.07	3.11	21.2	18.7

Table 2. Binding energy in the S_0 and S_1 states and transition energy calculated for the $M^+\cdot\text{DMB}$ complexes at the M05-2X/6-31+G(d) level with Stuttgart RLC potential for Rb and Cs.

M^+	Binding energy (eV)		Calculated transition energy (eV) ^a
	S_0	S_1	
Li ⁺	2.60	2.35	4.64
Na ⁺	1.82	2.50	4.61
K ⁺	1.25	1.69	4.56
Rb ⁺	0.75	0.63	4.52
Cs ⁺	0.62	0.52	4.51
(DMB monomer)	–	–	4.43

^aWe employ a scaling factor of 0.834 for the transition energy calculated. This factor is determined so as to reproduce the transition energy of DMB monomer.

Figure Captions

Figure 1. The UVPD spectra of the $M^+\bullet$ DMB ($M = \text{Li, Na, K, Rb, and Cs}$) complexes with the LIF spectrum of DMB reported by Pratt and coworkers (Ref. 19).

Figure 2. Expanded views of the UVPD spectra of the (a) $\text{K}^+\bullet$ DMB, (b) $\text{Rb}^+\bullet$ DMB, and (c) $\text{Cs}^+\bullet$ DMB complexes.

Figure 3. The IR-UV spectra of the $M^+\bullet$ DMB complexes in the CH stretching ($2800\text{--}3120\text{ cm}^{-1}$) region (solid curves). The IR spectra calculated for optimized structures (sticks). The calculated frequencies are multiplied by a scaling factor of 0.930 for comparison with the IR-UV spectra.

Figure 4. Top and side views of the $\text{Li}^+\bullet$ DMB complex in the S_0 state optimized at the M05-2X/6-31+G(d) level of theory.

Figure 5. Side views of the $\text{Li}^+\bullet$ DMB, $\text{Na}^+\bullet$ DMB, and $\text{K}^+\bullet$ DMB complexes in the S_0 and S_1 states optimized at the M05-2X/6-31+G(d) level.

Figure 6. The lowest-frequency normal mode of the $\text{Na}^+\bullet$ DMB complex in the S_0 state.

Figure 7. Fragment mass spectra of the Na⁺•DMB complex. These spectra are measured with a UV laser at 37220 cm⁻¹ (solid curve) and with no UV laser (dotted curve). The signal at $m/Z = 138$ is assigned to DMB⁺ ion.

Figure 8. The energy diagram of the Na⁺•DMB complex and related species. Numbers in the figure show the energy in eV. The binding energy between Na⁺ and DMB (1.82 eV) is obtained by the DFT calculations at the M05-2X/6-31+G(d) level.

References

- ¹ Y. Inokuchi, O. V. Boyarkin, R. Kusaka, T. Haino, T. Ebata and T. R. Rizzo, *J. Am. Chem. Soc.*, 2011, **133**, 12256–12263.
- ² C. J. Pedersen, *J. Am. Chem. Soc.*, 1967, **89**, 7017–7036.
- ³ D. Bright and M. R. Truter, *Nature*, 1970, **225**, 176–177.
- ⁴ D. Bright and M. R. Truter, *J. Chem. Soc. B*, 1970, 1544–1550.
- ⁵ M. A. Bush and M. R. Truter, *J. Chem. Soc. D*, 1970, 1439–1440.
- ⁶ M. A. Bush and M. R. Truter, *J. Chem. Soc. B*, 1971, 1440–1446.
- ⁷ N. S. Poonia and M. R. Truter, *J. Chem. Soc.-Dalton Trans.*, 1973, 2062–2065.
- ⁸ A. Bianchi, J. Giusti, P. Paoletti and S. Mangani, *Inorg. Chim. Acta*, 1986, **117**, 157–164.
- ⁹ V. A. Shubert, W. H. James and T. S. Zwier, *J. Phys. Chem. A*, 2009, **113**, 8055–8066.
- ¹⁰ V. A. Shubert, C. W. Muller and T. S. Zwier, *J. Phys. Chem. A*, 2009, **113**, 8067–8079.
- ¹¹ R. Kusaka, Y. Inokuchi and T. Ebata, *Phys. Chem. Chem. Phys.*, 2007, **9**, 4452–4459.
- ¹² R. Kusaka, Y. Inokuchi and T. Ebata, *Phys. Chem. Chem. Phys.*, 2008, **10**, 6238–6244.

- ¹³ R. Kusaka, Y. Inokuchi and T. Ebata, *Phys. Chem. Chem. Phys.*, 2009, **11**, 9132–9140.
- ¹⁴ T. R. Rizzo, J. A. Stearns and O. V. Boyarkin, *Int. Rev. Phys. Chem.*, 2009, **28**, 481–515.
- ¹⁵ A. Svendsen, U. J. Lorenz, O. V. Boyarkin and T. R. Rizzo, *Rev. Sci. Instrum.*, 2010, **81**, 073107 (7 pages).
- ¹⁶ O. V. Boyarkin, S. R. Mercier, A. Kamariotis and T. R. Rizzo, *J. Am. Chem. Soc.*, 2006, **128**, 2816–2817.
- ¹⁷ Gaussian 09, Revision A.02, M. J. Frisch, G. W. Trucks, H. B. Schlegel, G. E. Scuseria, M. A. Robb, J. R. Cheeseman, G. Scalmani, V. Barone, B. Mennucci, G. A. Petersson, H. Nakatsuji, M. Caricato, X. Li, H. P. Hratchian, A. F. Izmaylov, J. Bloino, G. Zheng, J. L. Sonnenberg, M. Hada, M. Ehara, K. Toyota, R. Fukuda, J. Hasegawa, M. Ishida, T. Nakajima, Y. Honda, O. Kitao, H. Nakai, T. Vreven, J. Montgomery, J. A., J. E. Peralta, F. Ogliaro, M. Bearpark, J. J. Heyd, E. Brothers, K. N. Kudin, V. N. Staroverov, R. Kobayashi, J. Normand, K. Raghavachari, A. Rendell, J. C. Burant, S. S. Iyengar, J. Tomasi, M. Cossi, N. Rega, J. M. Millam, M. Klene, J. E. Knox, J. B. Cross, V. Bakken, C. Adamo, J. Jaramillo, R. Gomperts, R. E. Stratmann, O. Yazyev, A. J. Austin, R. Cammi, C. Pomelli, J. W. Ochterski, R. L. Martin, K. Morokuma, V. G. Zakrzewski, G. A. Voth, P. Salvador, J. J. Dannenberg, S. Dapprich, A. D. Daniels, O. Farkas, J. B. Foresman, J. V. Ortiz, J. Cioslowski and D. J. Fox, Gaussian, Inc., Wallingford CT, 2009.

¹⁸ Schuchardt, K. L.; Didier, B. T.; Elsethagen, T.; Sun, L.; Gurumoorthi, V.; Chase, J.; Li, J.; Windus, T. L. *J. Chem. Inf. Model.* **2007**, *47*, 1045–1052.

¹⁹ J. T. Yi, J. W. Ribblett and D. W. Pratt, *J. Phys. Chem. A*, 2005, **109**, 9456–9464.

²⁰ NIST Chemistry WebBook, <http://webbook.nist.gov/chemistry/>.

²¹ Y. Mori, Y. Ogawa, H. Shinoda and T. Kitagawa, *Org. Mass Spectrom.*, 1992, **27**, 578–584.

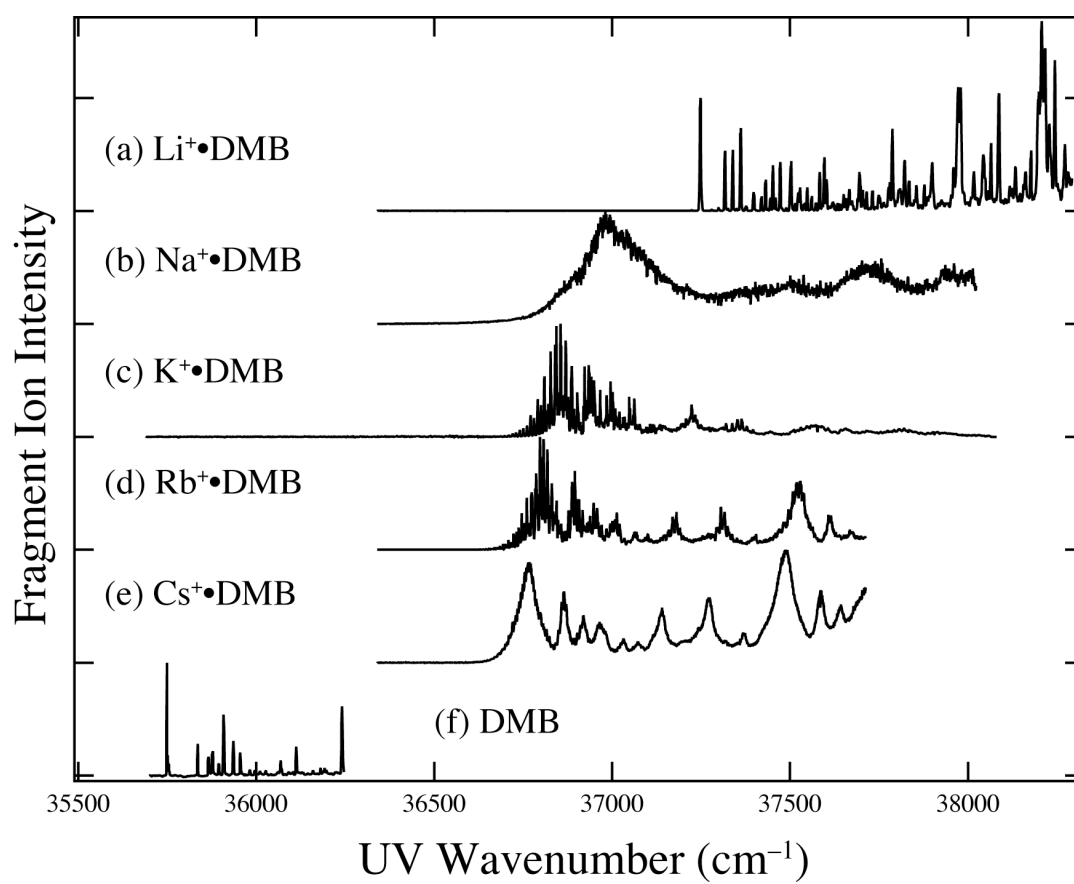


Figure 1. Inokuchi et al.

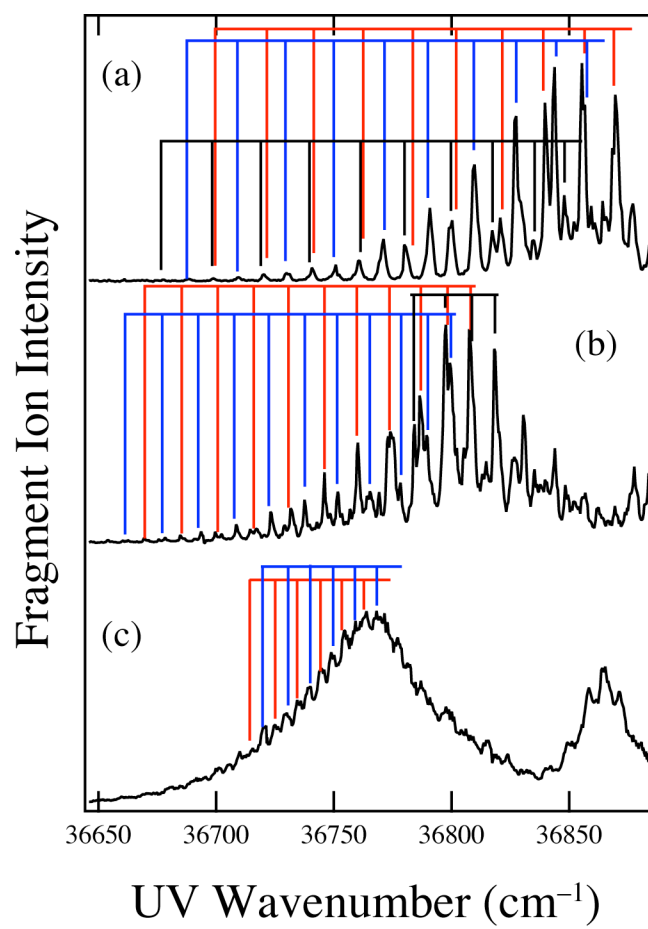


Figure 2. Inokuchi et al.

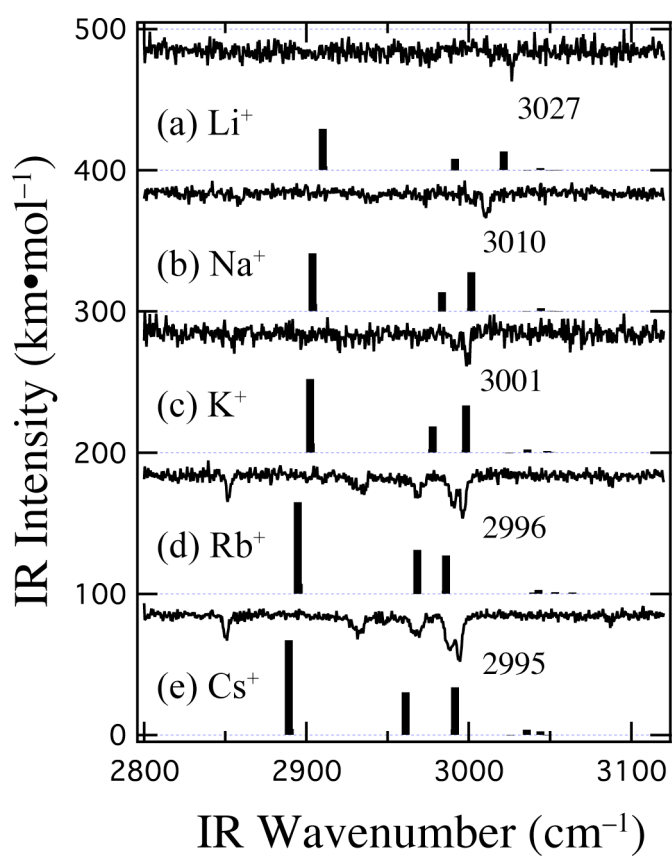


Figure 3. Inokuchi et al.

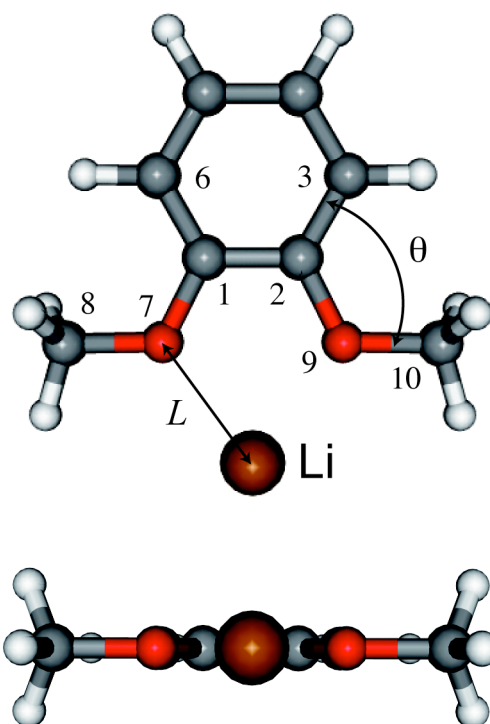


Figure 4. Inokuchi et al.

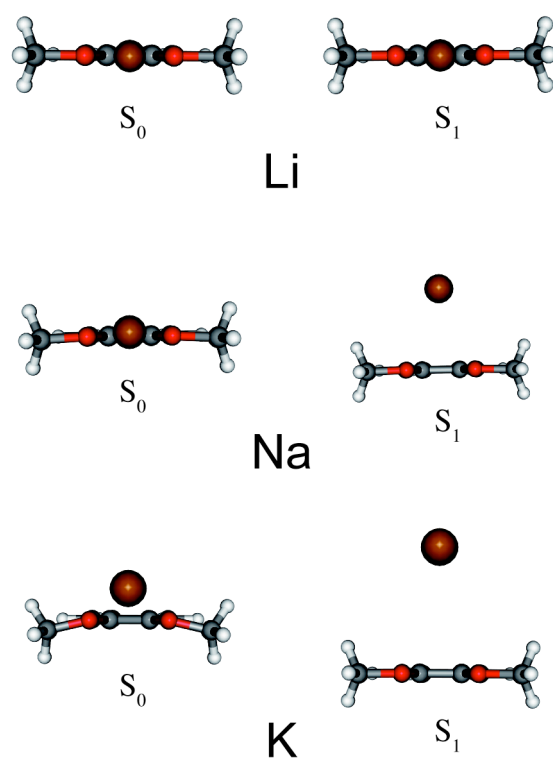


Figure 5. Inokuchi et al.

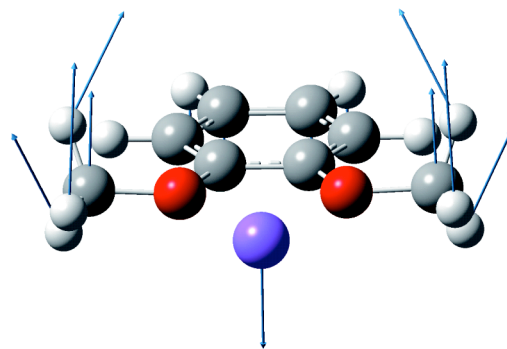


Figure 6. Inokuchi et al.

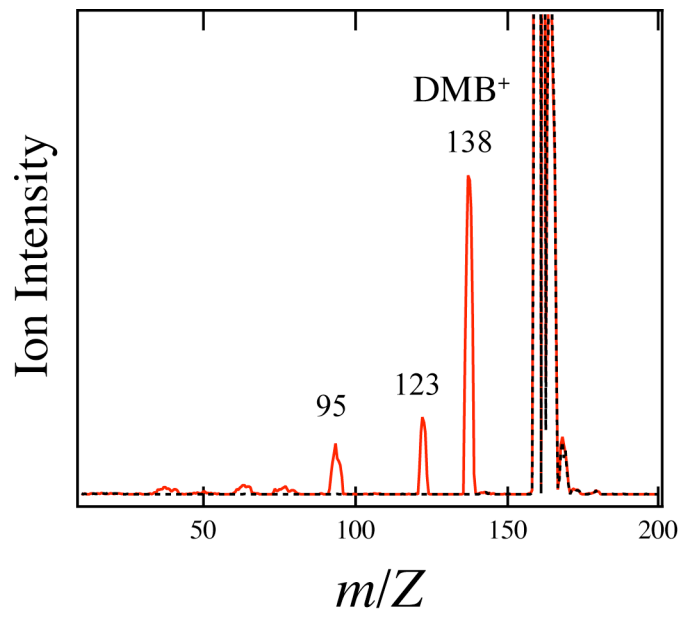


Figure 7. Inokuchi et al.

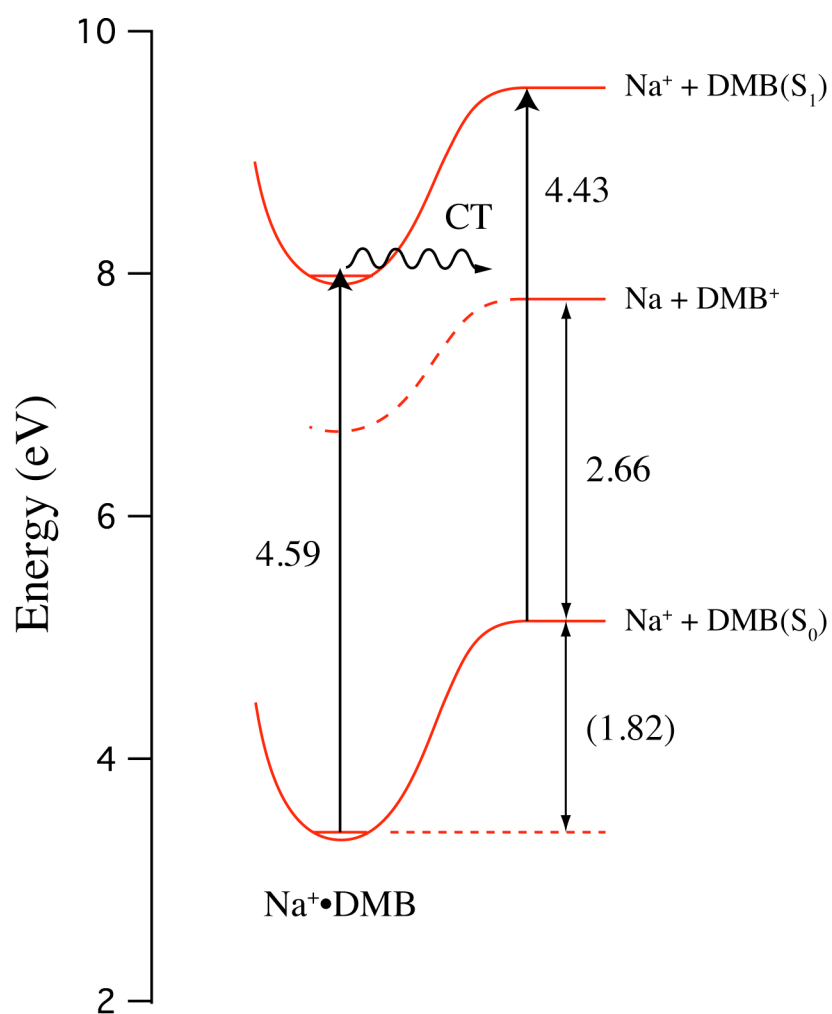
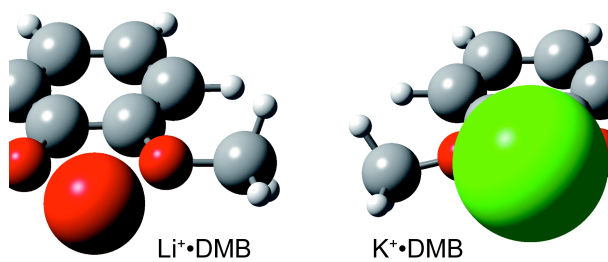


Figure 8. Inokuchi et al.

Table of contents



UV spectra of 1,2-dimethoxybenzene (DMB) complexes with alkali metal ions are measured in a cold, 22-pole ion trap, showing many well-resolved vibronic bands.